Phase diagrams of lyotropic cholesteric fluids

Pierre Tolédano,* A. M. Figueiredo Neto, and Z. A. de Sant'Ana†
Instituto de Física, Universidade de São Paulo, Caixa Postal 66318, 05315-970, São Paulo, SP, Brazil
(Received 19 July 1999)

Experimental investigations of lyotropic cholesterics fluids are presented which show that changes in the shape anisotropy and chirality of the micellar population determine the topology of the temperature-concentration phase diagrams. For given amounts of the substances which induce the chirality and modify the shape anisotropy of the micelles, two distinct biaxial cholesteric phases are disclosed in the phase diagrams. This is interpreted in the framework of the catastrophe theory of phase transitions.

PACS number(s): 64.70.Ja, 61.30.Gd

I. INTRODUCTION

The phase diagrams of lyotropic nematic fluids present specific features which are related to the fact that their building blocks, the micelles, undergo changes in their shape as functions of temperature and concentration [1]. One of the most remarkable features is the doubling of the singularities, within a given phase diagram, that was first observed by Yu and Saupe [2] in the lyotropic mixture of potassium laurate, decanol, and water ($KL/DeOH/D_2O$). In this system three distinct nematic phases are found, two uniaxial (denoted N_D and N_C) and one biaxial (N_B), which merge at a four-phase ''Landau'' point with the high-temperature isotropic phase (iso 1). Another isotropic phase (iso 2) takes place at lower temperature, and the second-order transition lines separating the N_D, N_B, and N_C phases seem to converge toward a second Landau point [2,3].

An analogous but more complex situation has been reported for lyotropic cholesteric systems, which are obtained for example by adding a chiral dopant to the nematic mesophases, such as brucine sulfate heptahydrate (BS) [4–7]. In the corresponding phase diagrams the N_D, N_B, and N_C phases are replaced by the chiral cholesteric variants, denoted Ch-*D*, Ch-*B*, and Ch-*C*, but the high-temperature Landau point can be either preserved [5] or substituted by two three-phase points [6,7]. In the low-temperature part of the phase diagram the second-order-transition lines separating the Ch-D, Ch-B, and Ch-C phases seem also to merge at a four-phase [5,6], or at two three-phase points [7].

The reentrance of the higher temperature isotropic phase (iso 1) below the nematic or cholesteric region (iso 2), and the reappearance of the singularities (four-or-three phase points) on the first-order transition line separating the preceding regions from the iso 2 phase has been interpreted, in the framework of the catastrophe theory of restructuring of phase diagrams [8], as a symmetric folding of the high-temperature region of the phase diagram induced by the change in micellar shape anisotropy with decreasing temperature [9,10]. There exists, however, in cholesteric systems another specific internal degree of freedom, the molecular chirality, that should also affect the topology of the phase diagrams, and has not been taken into account in the theoretical description of Refs. [9] and [10]. It has been shown, in this respect, that the pitch of the cholesteric structure is strongly dependent on the micellar anisometry [11].

The aim of the present article is twofold. At first we present the results of experimental investigations on lyotropic cholesteric systems (Sec. II), which reveal that the interplay between the chirality and anisometry of the micellar population determines in a decisive way the topology of the corresponding phase diagrams. In particular we show that for given amounts of the substances which induce the chirality and modify the shape anisotropy of the micelles, the phase diagram of the mixtures presents two distinct biaxial phases. Secondly, we analyze theoretically the topology of the experimental phase diagrams by extending the theoretical approach proposed in Refs. [9] and [10] (Sec. III). In Sec. IV we summarize our results and briefly discuss the conditions under which biaxial phases, which have been vainly searched in thermotropic liquid crystals [12], take place in lyotropic cholesteric fluids.

II. TEMPERATURE CONCENTRATION PHASE DIAGRAMS OF LYOTROPIC CHOLESTERIC MIXTURES

In a first series of experiments we investigated by optical techniques and x-ray diffraction, different mixtures of $KL/DeOH/H_2O/BS$. The study allowed us to work-out three types of phase diagrams having the characteristic topologies shown in Figs. 1(a)–1(e). In one type of phase diagrams [Fig. 1(a)] the relative molar concentration of BS is varied at fixed contents of DeOH, KL, and H_2O. The concentration of BS determines the chiral (twisting) field through the parameter $M_a=[BS]/([BS]+[DeOH]+[KL])$ where [ ] stands for the molar (percent) concentration. Varying M_a and the temperature T gives indications on the influence of the cholesteric pitch on the phase diagram topology for a given shape anisotropy of the micelles, determined by the contents of DeOH and KL. In another type of phase diagram [Figs. 1(b), 1(c), and 1(e)] the relative molar concentration between BS and H_2O is fixed while the value of the parameter $M_c=[DeOH]/([BS]+[DeOH]+[KL])$ is changed by varying the content of DeOH. It gives information on the influence of

*Permanent addresses: Groupe ''Structure des Matériaux sous Conditions Extrêmes'' SNBL/ESRF, BP220, 38043 Grenoble Cedex, France, and University of Amiens, Amiens, France.

†Permanent address: Instituto de Química, Universidade de São Paulo, São Paulo, Brazil.

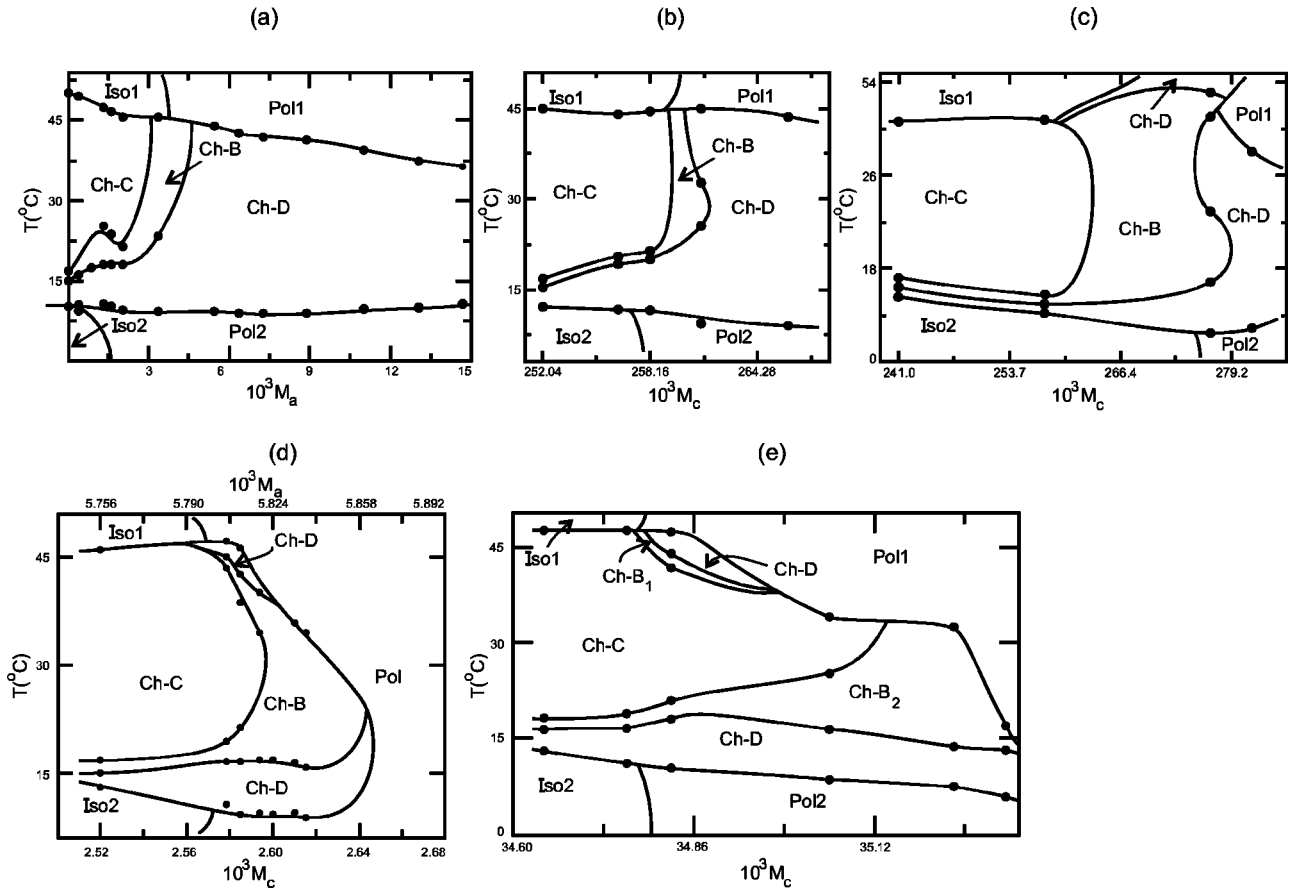

FIG. 1. (a)–(e) Phase diagrams obtained for different mixtures of KL/DeOH/H_2O/BS. The notation of the phases is defined in the text. M_a and M_c are dimensionless. The transition lines separating the phases represent a guide for the eye. (a) $M_c \simeq 37.13\times10^{-3}$. (b) and (c) $M_a \simeq 2.06\times10^{-3}$. (e) $M_a \simeq 5.72\times10^{-3}$.

the micellar shape anisotropy on the T-M_c phase diagram at fixed content of BS. In a third type of phase diagram [Fig. 1(d)] the values of M_a and M_c are simultaneously varied.

The optical and x-ray experimental setup, as well as the experimental procedures followed in our measurements, have been described in detail in Ref. [11]. The following information is obtained, which refer to the specific geometry of the optical experiment represented in Fig. 2.

(1) The usual three cholesteric phases (Ch-C, Ch-B, and Ch-D) are identified by their characteristic textures in a polarizing microscope. Since the Ch-D–Ch-B phase transition is not so easy to be determined by observing the textures, the corresponding transition temperatures are obtained by measuring the light transmittance I along the z axis as a function of temperature.

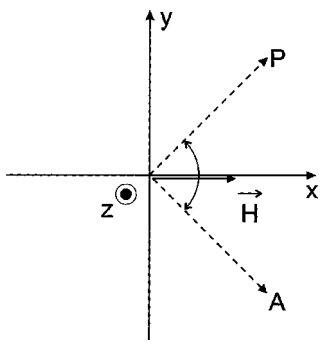

FIG. 2. Geometry of the optical experiment [11]. x, y, and z are the laboratory frame axes. $\vec{H}$ is the magnetic field used to orient the cholesteric (Ch-D and Ch-B) samples. P and A are the polarizer and the analyzer.

(2) The pitch P is determined by measuring I (at constant T) as a function of x along the helicoidal direction.

(3) The shape anisotropy $\mathcal{A}$ of the micelles is deduced from the x-ray diffraction patterns [11]. $\mathcal{A}$ is defined as the ratio between two typical micellar dimensions: the amphiphilic bilayer and the mean diameter of the micelles.

Concerning the dependences on T and relative concentrations M_a and M_c of the parameters P and $\mathcal{A}$, we could confirm the conclusions previously reached in Refs. [6,11,13,14]: namely (i) P *increases* with decreasing values of M_a (M_c fixed) and increasing temperature. The $P^{-1}(M_a)$ dependence is almost linear for the lower values of M_a and it deviates from linearity in the higher concentration limit. On the other hand P *decreases* linearly when M_c increases (M_a fixed). (ii) $\mathcal{A}$ *increases* almost linearly with increasing values of M_c (M_a fixed). (iii) $\mathcal{A}$ displays a nonmonotonous behavior with temperature. When T decreases $\mathcal{A}$ increases up to about the middle of the cholesteric region, then after reaching a maximum it decreases on approaching the low-temperature isotropic phase.

Figures 1(a)–1(e) represent the most typical phase diagrams obtained in this first series of experiments. They display a remarkable variety in the shapes of the different cho-

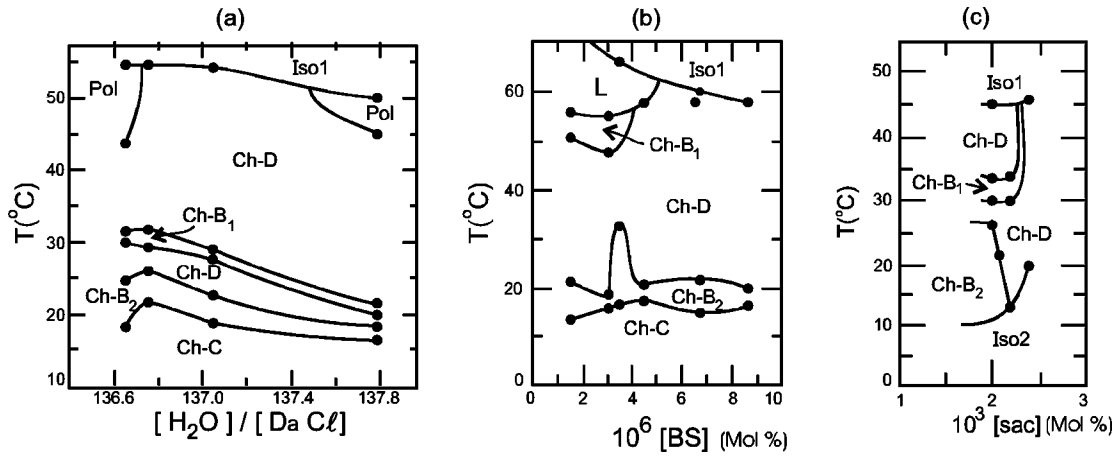

FIG. 3. Phase diagrams obtained for the mixtures KL/DaCl/H_2O/BS [(a) and (b)] and (Kl/KCl/DeOH/H_2O/Sac) (c). (a) $0.34<[\mathrm{BS}]<0.67$ and $0.0451<[\mathrm{DaCl}]<0.0906$. (b) $[\mathrm{DaCl}]/[\mathrm{KL}]=0.15$. In (c) $[\mathrm{DeOH}]/[\mathrm{KL}]=0.19$. In (b) *L* denotes a lamellar phase. [ ] stands for the molar (percent) concentration.

lesteric phases and in the type of singularities. The most striking feature is the variety of behaviors found for the shape of the biaxial Ch-*B* region in the phase diagrams and for the related singularities. In the high-temperature part of the phase diagrams, on the first-order transition line separating the iso 1 phase or polyphasic region (pol 1) from the cholesteric phase, the Ch-*B* phase merges with the other phases either at three-phase points [Figs. 1(a) and 1(b)] or at four-phase points [Figs. 1(c) and 1(d)]. Both types of points are present in the phase diagram of Fig. 1(e), in which the biaxial phase seems to split in two distinct regions of stability (a small one and a large one) denoted, respectively, Ch-B_1 and Ch-B_2. However, the actual configuration of the Ch-B_1 phase is uncertain since this phase occupies a narrow region of the phase diagram and is confirmed by only one data point. In contrast, the transition line separating the Ch-B_2 phase from the pol 1 region is clearly bounded by two three phases points.

In the low-temperature part of the phase diagrams of Figs. 1(a)–1(e), a very similar behavior is found for the biaxial phase in the low-concentration limit: the Ch-*C*–Ch-*B* and Ch-*D*–Ch-*B* second-order transition lines converge, in the direction of the iso 2 phase, toward a four-phase point. In some respects the preceding features realize a combination of the topologies found respectively for the biaxial nematic [2,3] and biaxial cholesteric [4,6] phases previously reported for lyotropic systems. Only in the phase diagram of Fig. 1(d) the shape of the Ch-*B* phase has the same topology previously found for a biaxial N_B phase [2,3].

In Figs. 1(a) and 1(b) the Ch-*C* and Ch-*D* phases occupy respectively the left and right hand sides of the phase diagram, the Ch-*D* phase remaining as the only stable phase at low temperature. In the three other phase diagrams the two uniaxial cholesteric phases exhibit a different configuration. In Figs. 1(c) and 1(d) the stability of the Ch-*D* phase is reduced by the extension of the Pol region which creates two distinct (small and large) regions of stability for the Ch-*D* phase. Three distict Ch-*D* phases surrounded by the Pol regions (denoted Pol 1 and Pol 2) appear in the phase diagram of Fig. 1(e). In contrast the Ch-*C* region of stability forms always a single phase across the different phase diagrams. It separates the two biaxial phases in Fig. 1(e).

In order to confirm the existence of two distinct biaxial phases in the phase diagram of lyotropic cholesteric systems and to precise the role played by the chiral dopant, a second series of experiments was undertaken. Two different types of cholesteric mixtures were investigated using the same experimental setup [11]. In one series of mixtures (KL/DaCl/H_2O/BS) we replaced DeOH by DaCl (decylammonium chloride) in order to modify the type of micellar anisometry [14]. In another series of mixtures (KL/KCl/DeOH/D_2O/Sac), potassium chlorate (KCl) is added and BS is replaced by Saccharose (Sac) inducing correlated modifications in the types of micellar shape anisotropy and chirality. Figures 3(a), 3(b), and 3(c) show the three phase diagrams in which the existence of two biaxial phases could be clearly confirmed. In the phase diagram of Fig. 3(a) the concentrations of DaCl and BS are both varied whereas only the concentrations of BS and Sac are changed in Figs. 3(b) and 3(c), respectively. Since our aim was mainly to find evidence of two separated biaxial phases in the same phase diagram, only reduced intervals of concentrations were explored. However, although these diagrams provide an incomplete picture of the phase boundaries the following features can be foreseen: (i) As in Fig. 1(e) the high-temperature biaxial (Ch-*B*1) phase occupies a more narrow region of stability than the low-temperature biaxial (Ch-*B*2) phase. (ii) At variance with the phase diagrams of Fig. 1 the Ch-*B*1 phase is only in contact with the Ch-*D* phase, and the Ch-*C* phase is here the most stable at low temperature [Figs. 3(a) and 3(b)] or is absent from the phase diagram [Fig. 3(c)].

III. PHENOMENOLOGICAL DESCRIPTION OF THE PHASE DIAGRAMS

In this section we first recall the basic ideas and formalism which have been used [9,10] to describe phase diagrams involving biaxial lyotropic phases (Sec. III A). We then extend this formalism in order to explain the possible stabilization of two biaxial phase in lyotropic cholesteric mixtures (Sec. III B) and the change in the type of singularities (three and four-phase points) found from one phase diagram to another (Sec. III C). At last, in Sec. III D, the variety of topological features revealed by the experimental phase diagrams

of Figs. 1 and 3, are shown to correspond to different situations predicted by the theoretical approach.

A. Topological metamorphosis

In Refs. [9] and [10] a theoretical model of the isotropic-nematic and isotropic-cholesteric phase transitions was proposed in which the modification of the shape of the micellar aggregates (which had been previously reported experimentally [15–18]) was taken into account. In this model the thermodynamic potential describing the phase diagrams which contain a biaxial phase can be written under the form

$$F_1(I_1,I_2,I_3)=a_1I_1+a_2I_1^2+b_1I_2+b_2I_2^2+c_1I_3+c_2I_3^2 + d_{12}I_1I_2+d_{13}I_1I_3+d_{23}I_2I_3+\cdots, \quad (1)$$

where I_1, I_2 and I_3 are the order-parameter invariants defined by

$$I_1(r,\tau)=r^2+\tau^2, \quad I_2(r,\theta)=r^3\cos 3\theta, \quad I_3(\tau)=\tau \quad (2)$$

and the (a_i,b_i,c_i,d_{ij}) are phenomenological coefficients which depend on temperature, but also on the number of micelles per unit volume. r and θ express, respectively, the deviations of the micellar shape from a sphere ($r=0$) and from a revolution ellipsoid ($\theta=0$). τ is a scalar (nonsymmetry breaking) order parameter representing the continuous change in shape of the micelles in function of temperature and concentration. In the framework of the theory of restructuring of phase diagrams, developed by Arnold [8,19], τ plays the role of an extravariable of the nonrigid internal degrees of freedom of the system which preserves the existing singularities and may lead to their multiplication. With respect to the current model of the isotropic-to-nematic phase transition proposed by Freiser [20] and Alben [21] [who used the two basic invariants $I_1(r)=r^2$ and $I_2(r,\theta)$] the variable τ introduces a new linear invariant $I_3(\tau)=\tau$ in the order-parameter expansion and results in a nonlinear transformation of the quadratic invariant:

$$I_1(r,\tau)=r^2+P^n(\tau), \quad (3)$$

where $P^n(\tau)$ is a polynomial of degree $n=2,3,4,\ldots,$ in τ. It may lead to a multiplication by n of the initial singularities, which is called [8,19] a topological metamorphosis.

In Ref. [9] the simplest quadratic form was considered [$P^n(\tau)=\tau^2$] to account for the reentrance of the isotropic phase and for the reappearance of the low-temperature four-phase point [2]. However, the existence of two biaxial phases and the variety of behaviors for the singularities found in the phase diagrams of Figs. 1 and 3 reveals a complex situation which requires a more elaborated theoretical scheme.

B. Influence of chirality

The existence of two distinct biaxial regions in the phase diagrams of Figs. 1(e) and 3(a), 3(b), 3(c) suggests *a priori* that a ''double'' topological metamorphosis occurs that may be described phenomenologically by a third degree polynomal ($n=3$) in Eq. (3). However, one can show that this would imply also a double reentrance of the high-temperature isotropic phase, and a number of constraints on the topology of the uniaxial and biaxial phases, as well as on the corresponding singularities, which are not observed experimentally. A more consistent description of the phase diagrams of Figs. 1 and 3 can be made by taking into account the chiral nature of the cholesteric mixtures, i.e., to assume that the chirality of the micellar population requires to introduce in the theoretical approach an additional internal degree of freedom.

The theoretical description of chiral liquid crystal phases is usually taken into account via a pseudoscalar order parameter which allows existence of inhomogeneous gradient terms [22]. However, when aiming to describe only the topology of the phase diagram, and not the inhomogeneous character of some of the phases, it is sufficient to consider the homogeneous order-parameter invariants. One can express here the influence of chirality via the pseudoscalar normalized quantity

$$\frac{\nu}{\nu_0}=\frac{P_0}{P}, \quad (4)$$

where P is the helical pitch deduced from light transmittance measurements (see Sec. II) and $\nu_0=1/P_0$, where P_0 is the maximal value of the pitch measured just below the iso 1 phase. ν/ν_0 is a normalized dimensionless variable, varying from -1 to $+1$, where the negative values are arbitrarily assumed to correspond to left handed helices and $\nu/\nu_0\geqslant 0$ coincides with righ-handed helices. In the framework of the theory of restructuring of phase diagrams, the effect of the nonsymmetry breaking order parameter ν/ν_0 is to introduce an additional linear invariant

$$I_4=\frac{\nu}{\nu_0} \quad (5)$$

and to produce a nonlinear transformation of the quadratic invariant, which will be taken as

$$I_1'(r,\tau,\nu)=r^2+\tau^2+\left(\frac{\nu}{\nu_0}\right)^2. \quad (6)$$

Accordingly the thermodynamic potential associated with the four-component (reducible) order parameter $(r,\theta,\tau,\nu/\nu_0)$ is

$$F_2(I_1',I_2,I_3,I_4)=F_1(I_1',I_2,I_3)+e_1I_4+e_2I_4^2+d_{14}I_1'I_4 + d_{24}I_2I_4+d_{34}I_3I_4. \quad (7)$$

Standard minimization of F_2 with respect to the different variables yields phase diagrams, which contain the different uniaxial and biaxial lyotropic cholesteric phases, as well as the two isotropic (iso 1 and iso 2) phases. Figure 4 shows the location of the three cholesteric and two isotropic phases in the three-dimensional space of the invariants (I_2,I_3,I_4). One can see that the region of stability of the biaxial Ch-*B* phases, occupies the interior of a ''flying saucer'' type volume ($-1<\cos 3\theta<1$) limited by the Ch-*C* and Ch-*D* surfaces ($\cos 3\theta=\pm 1$). The isotropic phases correspond to the bounding circle defined by $r=0$, $\tau^2+(\nu/\nu_0)^2=1$, and $-1<\tau<+1, -1<(\nu/\nu_0)<+1$. The same figure represents the variation of the preceding volume along the I_1' axis. It shows

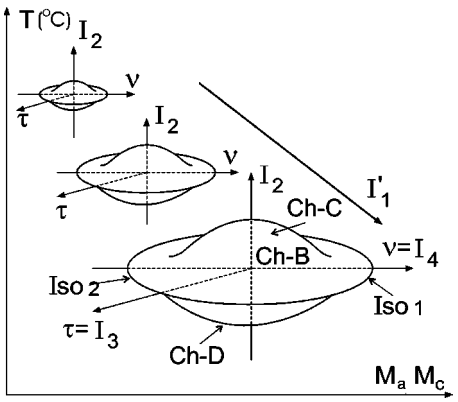

FIG. 4. Configuration of the regions of stability of the cholesteric and isotropic phases in the 3D space of the invariants (I_2, I_3, I_4), and evolution of the corresponding volume along the I_1' axis, and with T, M_a, and M_c.

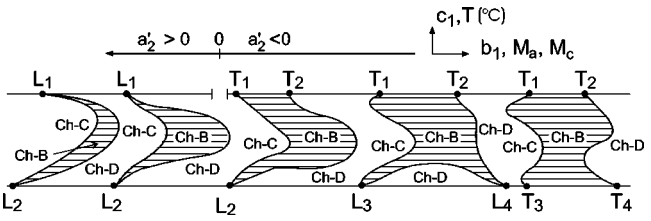

FIG. 5. Evolution of the shape of the biaxial phase when the phenomenological coefficient a_2' defined by Eq. (8) is varied, under the condition $4a_2'b_2 - d_{12}^2 > 0$. The evolution is shown in the plane (c_1, b_1), or equivalently in the $[T, (M_a \text{ or } M_c)]$ plane. A topological transition occurs when L_1 is transformed in (T_1, T_2) or when L_2 transforms into (L_3, L_4).

that when I_1' increases [i.e., for increasing values of the r, τ or (ν/ν_0) parameters] one gets sucessive inflated self-similar volumes. Coming back to the experimental phase diagrams, which are two-dimensional *nonlinear cross sections* of the four-dimensional space (I_1', I_2, I_3, I_4), one can interpret the regions of stability of two distinct biaxial phases as cross sections of two distinct hypervolumes represented symbolically in Fig. 4.

In Sec. II it has been concluded from the experiments that an increase of M_c corresponds to an increase of the shape anisotropy $\mathcal{A}$ and to a decrease of the helical pitch P. Therefore the three variables r, τ, and ν/ν_0 *increase* with increasing M_c and, since I_1' increases, contribute to an enlargement of the hypervolume symbolizing the biaxial cholesteric region in Fig. 4. This is consistent with the larger surface occupied by the Ch-B_2 phase with respect to the Ch-B_1 phase in Fig. 1(e), as it occurs for larger values of M_c and thus coincides with a cross-section of a larger hypervolume. The same conclusion holds for the Ch-B_2 and Ch-B_1 phases in Figs. 3(a) and 3(b).

As noted in Sec. II, P decreases (and ν/ν_0 increases) with decreasing temperature and should contribute to an increase of I_1' at lower temperatures, i.e., of the surface of the phase diagram occupied by the biaxial region. At variance $\mathcal{A}$ (and therefore r, τ, and I_1') increases with decreasing temperature only in the central part of the cholesteric region. This is in qualitative agreement with the shape of the biaxial region, as observed in Figs. 1(b) and 1(d), which enlarges at middle distance from the iso 1 and iso 2 phases, but reduces close to those phases. It is also consistent with the enlargement of the Ch-B_2 phase with respect to the high-temperature Ch-B_1 phases, shown in Fig. 1(e) and Figs. 3(a), 3(b), 3(c).

C. Transformation of the singularities

Another remarkable feature of the experimental phase diagrams of Figs. 1 and 3 is not accounted for in the preceding description, namely, the change in the nature of the singularities connecting the biaxial phase to the isotropic or polyphasic (pol 1, pol 2, pol) phases. Thus in the phase diagrams of Figs. 1(a), 1(b), and 1(c) the Ch-B phase connects with the iso 1 and pol 1 phases at two three-phases points and converges towards the iso 2 phase at a four-phase point. In Fig. 1(d) the Ch-B phase is closed by two four-phase points lying, respectively, on the boundaries of the iso 1 and iso 2 phases. In Fig. 1(e) the Ch-B_2 phase merge with the pol 1 and Ch-C phases at a triple point, and seem to converge towards the iso 2 and pol 2 phases at two four-phase points. This variety of situations is related to the property, shown in Refs. [9] and [10], that the shape of the biaxial regions and the corresponding types of singularities depend on the sign of the phenomenological coefficient a_2 in Eq. (1): For $a_2 > 0$ the biaxial phase has been shown in Ref. [10] to display a ''moon-section'' type of shape ending at two four-phase (Landau) points, whereas for $a_2 < 0$ the shape is modified and exhibits three-phase points [10].

Let us show that changes in the values of τ and (ν/ν_0) may induce a change in sign of a_2 and consequently produce a change in the shape of the biaxial phase (s) and of the corresponding n-phase points. Minimizing F_2 with respect to τ and (ν/ν_0) yields the equilibrium values $\tau^2 \simeq -(1/2c_2)(c_1 + d_{13}I_1')$ and $\nu^e/\nu_0 = -(1/2e_2)(e_1 + d_{14}I_1')$. Hence, the quadratic contribution to F_2 which is $c_2(\tau^e)^2 + e_2(\nu^e/\nu_0)^2$ leads to a renormalization of the coefficient of $I_1'^2$ which is

$$a_2' = a_2 + \frac{1}{4}\left(\frac{d_{13}^2}{c_2} + \frac{d_{14}^2}{e_2}\right). \tag{8}$$

Accordingly a_2' may have either the sign of a_2 or the reverse sign depending on the respective signs and values of c_2 and e_2, and on the magnitude of the coupling coefficients d_{13} and d_{14}. In other words, varying the micellar shape anisotropy (τ) and the chirality (ν/ν_0) may give rise to different topologies for the biaxial cholesteric phase. This is illustrated in Fig. 5 which shows the evolution of the shape of the preceding phase when a_2' varies from positive to negative values. For $a_2' = 0$ the Landau point L_1 transforms into two triple points T_1 and T_2 on the first-order transition line separating the iso 1 phase from the cholesteric region. Note that on the first-order transition line separating the iso 2 phase from the preceding region the change in the topology of the singular points (from a four-phase to a three-phase point) may not occur simultaneously since at lower temperature the shape anisotropy and chirality are different and the coefficients c_2, e_2, d_{13}, and d_{14} have different values. Note also that the

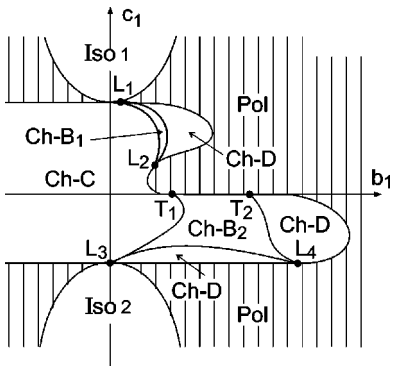

FIG. 6. Theoretical phase diagram in the (c_1,b_1) plane reflecting the double topological metamorphosis and topological transition described in the text.

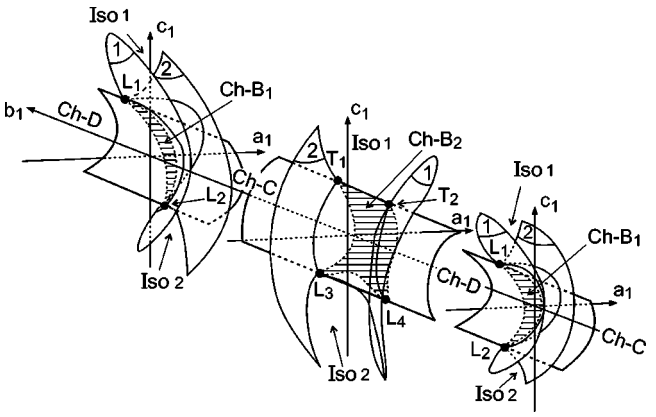

FIG. 7. Theoretical phase diagram in the (c_1,b_1,a_1) space. The biaxial phase shown in the central figure $(a_2'<0)$ is stabilized at lower temperature and larger concentrations (M_a,M_c) than the biaxial phases represented in the left- or righ-hand side figures $(a_2'>0)$. The surfaces denoted 1 and 2 are the limit of stability of the isotropic phases.

transformation from four-phase-to three phase points may occur via an intermediate stage involving two four-phase points.

D. Crossover from simple to double topological metamorphosis

Figure 6 represents the combined effect of the preceding transformations in the plane of the phenomenological coefficients (c_1,b_1). It shows two distinct regions of stability for the biaxial phase, one being inflated with respect to the other toward lower temperatures and larger concentrations. On the other hand the shape of the two biaxial phases is topologically transformed by a change in the sign of the coefficient a_2' with decreasing temperature and increasing concentration M_c. Assuming a linear dependence of c_1 and b_1 as functions of T and M_c, the theoretical phase diagram of Fig. 6 reflects the essential features of the experimental phase diagram of Fig. 1(e), which can therefore be understood as exhibiting a *double topological metamorphosis* of the high-temperature singularity (four-phase point) as well as a *topological transition* changing the shape of the biaxial phase. This interpretation seems also to hold for the phase diagrams of Figs. 3(b) and 3(c), although the existing singularities are only partly singled out. In contrast the phase diagrams of Figs. 1(a), 1(b), 1(c), and 1(d) correspond to a simple topological metamorphosis occurring with [Figs. 1(a), 1(b), and 1(c)] or without [Fig. 1(d)] a change in the nature of the singularities. Note that in Fig. 6 there exists three separated regions of stability for the Ch-*D* phase, and only one Ch-*C* phase, whereas in the experimental phase diagram of Fig. 1(e) two distinct Ch-*D* regions are found. Note also that the symmetry of the theoretical phase diagram with respect to the b_1 and c_1 axes, which had been pointed out in Refs. [9] and [10] as typifying a single topological metamorphosis, is here lost except for the iso 1 and iso 2 phases.

Figure 7 represents the simultaneous effects of a double topological metamorphosis of the four-phase point L_1 (which gives rise to the L_2, T_1, T_2, L_3, and L_4 points) and of a topological transformation of the biaxial phase (a_2' going from positive to negative values) in the 3D space (a_1,b_1,c_1). Thus, one may have either two biaxial phases separated by the Ch-*C* phase, with a low-temperature Ch-*D* phase, as in the phase diagram of Fig. 1(e), or two biaxial phases separated by the Ch-*D* phase, with a low temperature Ch-*C* phase as in the phase diagrams of Figs. 3(a) and 3(b).

IV. SUMMARY AND CONCLUSION

In summary, we have presented experimental phase diagrams of lyotropic cholesteric fluids, which reveal a remarkable variety of configurations with respect to the phase diagrams previously obtained for such systems [4–7]. The most striking result is the observation in some of the obtained phase diagrams of two distinct biaxial phases, as well as two or three distinct uniaxial Ch-*D* phases. The fact that the respective influences of the shape anisotropy and chirality of the micellar population on the stabilization of the various cholesteric phases cannot be clearly separated, and the contrasted topologies found in the different phase diagrams, do not allow a simple picture of the conditions under which biaxial phases may form. However, analyzing the experimental phase diagrams of Figs. 1 and 3 suggests the following remarks. From the phase diagrams of Figs. 1(a) and 1(b) the biaxial phase appears as corresponding to an intermediate regime between the uniaxial Ch-*C* and Ch-*D* cholesteric phases, which take place, respectively, for small and large values of both the micellar shape anisotropy and chirality. This is confirmed in the phase diagram of Fig. 1(e) where the two biaxial phases are again bounded by the Ch-*C* and Ch-*D* phases. A prerequisite for the existence of the second (Ch-$B1$) biaxial phase being the stabilization of a second uniaxial Ch-*D* phase, which appears in the upper part of the phase diagrams of Figs. 1(c), 1(d), and 1(e). In those phase diagrams the variational parameter which seems to discriminate the high- and low-temperature Ch-*D* and Ch-B_1–Ch-B_2 phases is the chiral-order parameter. However, the phase diagrams shown in Fig. 3 confirm only partly the preceding conclusions. Thus if the Ch-B_2 phase is again bounded by a Ch-*D* and Ch-*C* phase in Figs. 3(a) and 3(b), the Ch-B_1 phase is sandwiched by two Ch-*D* phases [Figs. 3(a) and 3(c)] or by a lamellar phase and a Ch-*D* phase [Fig. 3(b)].

A theoretical description has been proposed to relate the observed features of the phase diagrams to the conjuncted

influences of changes in the shape anisotropy and chirality of the micelles. With respect to a previous theoretical approach of the phase diagrams of lyotropic nematic and cholesteric phase diagrams [9,10], it takes explicitly into account the chirality as an additional internal degree of freedom of the system. Accordingly the difference in the size and location of the two biaxial phases are interpreted as two different nonlinear two-dimensional cross sections of a hypervolume of the order-parameter space. On the other hand the modification in the nature of the corresponding singularities (three- or four-phase points) has been related to a change in sign of one of the phenomenological coefficients in the order-parameter expansion, which can be induced by a change in the shape anisotropy and chirality of the micellar population.

ACKNOWLEDGMENT

Fundação de Amparo à Pesquisa do Estado de São Paulo supported this work.

[1] A.M. Figueiredo Neto, in *Phase Transitions in Complex Fluids*, edited by P. Tolédano and A.M. Figueiredo Neto (World Scientific, Singapore, 1998) p. 151.
[2] L. Yu and A. Saupe, Phys. Rev. Lett. **45**, 1000 (1980).
[3] E.A. Oliveira, L. Liébert, and A.M. Figueiredo Neto, Liq. Cryst. **5**, 1669 (1989).
[4] A.M. Figueiredo Neto, Y. Galerne, and L. Liébert, J. Phys. Chem. **89**, 3939 (1985).
[5] G. Melnik and A. Saupe, Mol. Cryst. Liq. Cryst. **145**, 95 (1987).
[6] A.M. Figueiredo Neto and M.E. Marcondes Helene, J. Phys. Chem. **91**, 1466 (1987).
[7] M.E. Marcondes Helene and A.M. Figueiredo neto, Mol. Cryst. Liq. Cryst. Sci. Technol., Sect. B **162**, 127 (1988).
[8] V.I. Arnold, A.N. Varchenko, and S.M. Gusein-Zade, *Singularities of Differential Maps* (Birkhauser, Boston, 1985), Vols. 1 and 2.
[9] P. Tolédano and A.M. Figueiredo Neto, Phys. Rev. Lett. **73**, 2216 (1994).
[10] P. Tolédano, A.M. Figueiredo Neto, V. Lorman, B. Mettout, and V. Dmitriev, Phys. Rev. E **52**, 5040 (1995).
[11] M.C. Valente Lopes and A.M. Figueiredo Neto, Phys. Rev. A **38**, 1101 (1988).
[12] See, for example, Liq. Cryst. Today **7**, 4 (1997).
[13] L. Yu and A. Saupe, J. Am. Chem. Soc. **102**, 4879 (1980).
[14] A.M. Figueiredo Neto, L. Liébert, and A.M. Levelut, J. Phys. (Paris) **45**, 1505 (1984).
[15] Y. Galerne, A.M. Figueiredo Neto, and L. Liébert, J. Chem. Phys. **87**, 1851 (1987).
[16] A.M. Figueiredo Neto, Y. Galerne, A.M. Levelut, and L. Liébert, J. Phys. (France) Lett. **46**, L499 (1985).
[17] A.M. Figueiredo Neto, Y. Galerne, and L. Liébert, Liq. Cryst. **10**, 751 (1991).
[18] Y. Galerne, A.M. Figueiredo Neto, and L. Liébert, Phys. Rev. A **31**, 4047 (1985).
[19] V.I. Arnold, Commun. Pure Appl. Math. **29**, 557 (1976).
[20] M.J. Freiser, Phys. Rev. Lett. **24**, 1041 (1970).
[21] R. Alben, Phys. Rev. Lett. **30**, 778 (1973).
[22] H. Pleiner and H.R. Brand, Phys. Rev. Lett. **54**, 1817 (1985).